



# **Low-cost Electronically Scanning Antenna with Randomly Selected Delay Line Lengths**

**by Geoffrey Goldman**

**ARL-TR-5211**

**June 2010**

## **NOTICES**

### **Disclaimers**

The findings in this report are not to be construed as an official Department of the Army position unless so designated by other authorized documents.

Citation of manufacturer's or trade names does not constitute an official endorsement or approval of the use thereof.

Destroy this report when it is no longer needed. Do not return it to the originator.

# **Army Research Laboratory**

Adelphi, MD 20783-1197

---

---

**ARL-TR-5211**

**June 2010**

---

## **Low-cost Electronically Scanning Antenna with Randomly Selected Delay Line Lengths**

**Geoffrey Goldman**  
**Sensors and Electron Devices Directorate, ARL**

REPORT DOCUMENTATION PAGE			Form Approved OMB No. 0704-0188		
<p>Public reporting burden for this collection of information is estimated to average 1 hour per response, including the time for reviewing instructions, searching existing data sources, gathering and maintaining the data needed, and completing and reviewing the collection information. Send comments regarding this burden estimate or any other aspect of this collection of information, including suggestions for reducing the burden, to Department of Defense, Washington Headquarters Services, Directorate for Information Operations and Reports (0704-0188), 1215 Jefferson Davis Highway, Suite 1204, Arlington, VA 22202-4302. Respondents should be aware that notwithstanding any other provision of law, no person shall be subject to any penalty for failing to comply with a collection of information if it does not display a currently valid OMB control number.</p> <p><b>PLEASE DO NOT RETURN YOUR FORM TO THE ABOVE ADDRESS.</b></p>					
1. REPORT DATE (DD-MM-YYYY) June 2010		2. REPORT TYPE Final		3. DATES COVERED (From - To)	
4. TITLE AND SUBTITLE Low-cost Electronically Scanning Antenna with Randomly Selected Delay Line Lengths			5a. CONTRACT NUMBER		
			5b. GRANT NUMBER		
			5c. PROGRAM ELEMENT NUMBER		
6. AUTHOR(S) Geoffrey Goldman			5d. PROJECT NUMBER		
			5e. TASK NUMBER		
			5f. WORK UNIT NUMBER		
7. PERFORMING ORGANIZATION NAME(S) AND ADDRESS(ES) U.S. Army Research Laboratory ATTN: RDRL-SES-P 2800 Powder Mill Road Adelphi, MD 20783-1197			8. PERFORMING ORGANIZATION REPORT NUMBER  ARL-TR-5211		
9. SPONSORING/MONITORING AGENCY NAME(S) AND ADDRESS(ES)			10. SPONSOR/MONITOR'S ACRONYM(S)		
			11. SPONSOR/MONITOR'S REPORT NUMBER(S)		
12. DISTRIBUTION/AVAILABILITY STATEMENT Approved for public release; distribution unlimited.					
13. SUPPLEMENTARY NOTES					
14. ABSTRACT A radar architecture that requires a single analog-to-digital converter and no active phase shifters was developed that can electronically search a three-dimensional (3-D) volume and provide range resolution and angular resolution proportional to the Rayleigh criterion for a given bandwidth and aperture size. The architecture is based on a frequency scanning antenna feed with delay lines whose lengths are randomly selected in combination with digital signal processing algorithms. I investigated the feasibility of the architecture to perform target localization in position and velocity by analyzing one-dimensional (1-D) antenna patterns and graphing a cost function based on an $L_2$ -norm. A single realization of the system was selected, simulated, and analyzed. The range and velocity resolution seen in the plots of two-dimensional (2-D) slices of the cost function are consistent with the position and velocity resolution derived from the Rayleigh criterion. For a low-cost solution, signals with Doppler shifts that exceed a given threshold should be transmitted to a central computer for more processing.					
15. SUBJECT TERMS ESA radar scanning antenna					
16. SECURITY CLASSIFICATION OF:			17. LIMITATION OF ABSTRACT  UU	18. NUMBER OF PAGES  26	19a. NAME OF RESPONSIBLE PERSON Geoffrey Goldman
a. REPORT Unclassified	b. ABSTRACT Unclassified	c. THIS PAGE Unclassified			19b. TELEPHONE NUMBER (Include area code) (301) 394-0882

---

## Contents

---

<b>List of Figures</b>	<b>iv</b>
<b>Acknowledgments</b>	<b>v</b>
<b>1. Introduction</b>	<b>1</b>
<b>2. Radar System</b>	<b>2</b>
<b>3. 1-D Antenna Patterns</b>	<b>3</b>
<b>4. Simulation</b>	<b>7</b>
<b>5. Cost Function</b>	<b>11</b>
<b>6. Conclusions</b>	<b>14</b>
<b>7. References</b>	<b>16</b>
<b>List of Symbols, Abbreviations, and Acronyms</b>	<b>17</b>
<b>Distribution List</b>	<b>18</b>

---

## List of Figures

---

Figure 1. Block diagram of radar system with feed lines for the receive antenna whose length are selected randomly. ....	2
Figure 2. Two-dimensional (2-D) geometry for a 1-D linear array for a stationary target in the far-field.....	3
Figure 3. The 1-D receive antenna patterns for the first, second, and fifth frequency step.....	7
Figure 4. Eigenvalues of the observation matrix created from the different antenna patterns. ....	8
Figure 5. Simulated 1-D antenna pattern using matched filter and WLSQ approaches. ....	8
Figure 6. The 1-D antenna patterns simulated for SNRs of 10, 20, and 25 dB. ....	10
Figure 7. Zoomed in 1-D antenna patterns simulated for SNRs of 10, 20, and 25 dB. ....	10
Figure 8. Cost function for a single target located at (5,0) m. ....	12
Figure 9. Cost function zoomed in for a single target located at (5,0) m. ....	13
Figure 10. Cost function for a single target with a velocity vector of (15,15) m/s.....	13
Figure 11. Cost function zoomed in for a single target with a velocity vector of (15,15) m/s.....	14

---

## **Acknowledgments**

---

I would like to thank Amir Zaghoul for his helpful discussions on the antenna configuration and signal processing algorithms and Theo Anthony for his helpful discussions on antenna configurations.

INTENTIONALLY LEFT BLANK.

---

## 1. Introduction

---

Moving target indicator (MTI) radars have been used to detect and track targets since World War II. When searching for targets, a narrow antenna beam is typically scanned through a large region of interest. For most operational radar systems, the beam is scanned by rotating an antenna on a gimbal (1). For more recently developed systems, the beam is scanned electronically with a phased array antenna using switches, ferroelectrics, or other active devices. Phased array antennas can be expensive and consume large amounts of power. Another less expensive approach for scanning a radar beam is to use a frequency scanning antenna. Systems using frequency scanning antennas trade good angular resolution for poor range resolution (2). The goal of this design is to have a low-cost, low-power system with both good range and angular resolution.

Numerous techniques have been developed to reduce the cost, size, and power requirements of electronically scanning antennas (ESA). One technique to reduce the cost is to aperiodically place a smaller number of antenna elements across an aperture (3). This technique has been shown to be feasible based on performance metrics such as peak sidelobe level (4). I am proposing a similar concept but different implementation for reducing the cost of the system. My proposal is a radar system architecture based on a frequency scanning antenna with delay lines whose lengths are deterministic, but randomly selected, in combination with digital signal processing algorithms. This architecture uses temporal diversity rather than spatial diversity to reduce the cost and improve the performance on the system.

Conceptually, orthogonal beam patterns at the receive antenna will be generated at each frequency with varying levels of energy spread spatially across the single element antenna pattern. Then, signal processing algorithms based on techniques such as least squares and maximum likelihood will be used to detect and track the targets of interest. From information theory, the maximum information content of a signal is obtained when the data have a uniform distribution and minimum information content is obtained when the data have a delta-like distribution (5). Traditionally, antenna patterns are delta-like functions, which are scanned across a field of view. More information about the targets should be obtained using a series of patterns that have distributions more closely resembling a uniform distribution.

This report examines the feasibility of an architecture based upon a one-dimensional (1-D) linear array feed with random length lines. The major advantages of the architecture are a simple radar RF design, an antenna with no active elements, and a data acquisition system comprised of a single slow-speed analog-to-digital converter (ADC). The major disadvantages of the architecture are the signal processing is much more complicated, the effective signal processing gain associated with the antenna may be reduced relative to a similarly sized antenna, and there are potential ambiguities associated with target localization.

---

## 2. Radar System

---

A radar architecture with a single input and single output was developed with the goal of having near orthogonal beams as a function of frequency in the receive antenna. The concept supports arbitrary waveforms and arbitrary antenna placement; however, to simplify the signal processing, a radar system based upon a continuous wave (CW) stepped-frequency waveform was analyzed. Figure 1 shows a block diagram of the radar system. The radar signal is transmitted through a single antenna and received with an array of antennas that are combined with feed lines of random length. The received signal is amplified, down converted, and then smoothed with a band-pass filter (BPF). Only signals from targets moving at a sufficient velocity will pass to the ADC. The single element antenna patterns for both transmit and receive antenna elements are identical.

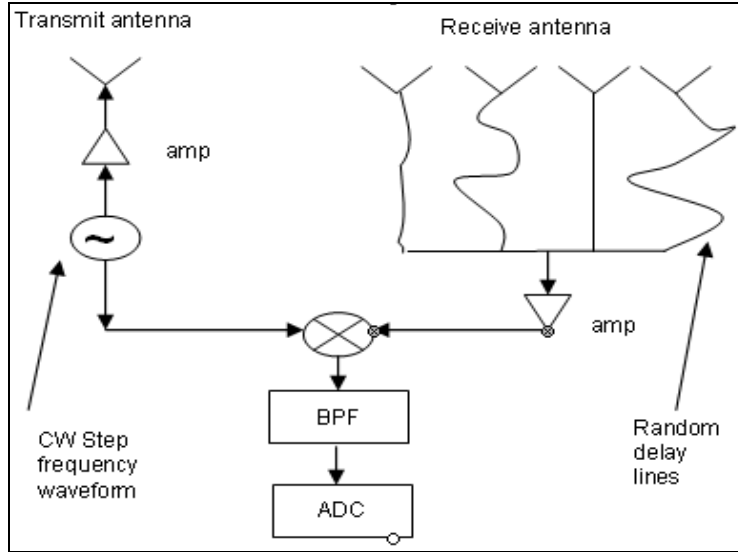


Figure 1. Block diagram of radar system with feed lines for the receive antenna whose length are selected randomly.

Conceptually, the proposed radar system contains enough information to track moving targets in stationary clutter. The velocity of the targets can be determined by performing a discrete Fourier transform (DFT) on the time samples collected at each frequency. Conceptually, the range information on moving targets can be obtained by performing a DFT across the Doppler-processed results after motion compensation and windowing. Conceptually, the angle of the targets can be determined using techniques such as matched filter processing or least squares estimation. To estimate target parameters, stochastic optimization techniques need to be developed. This report studies the feasibility of estimating the target parameters by analyzing a cost function based upon the Euclidian norm.

### 3. 1-D Antenna Patterns

Analysis of the 1-D antenna patterns provides insight into the more complicated system identification problem. 1-D antenna patterns were simulated and analyzed for a radar system similar to the block diagram shown in figure 1. For stationary targets, the BPF shown in figure 1 was removed. The geometry associated with a 1-D array with  $N$  antenna elements for the  $p$ th target is shown in figure 2.

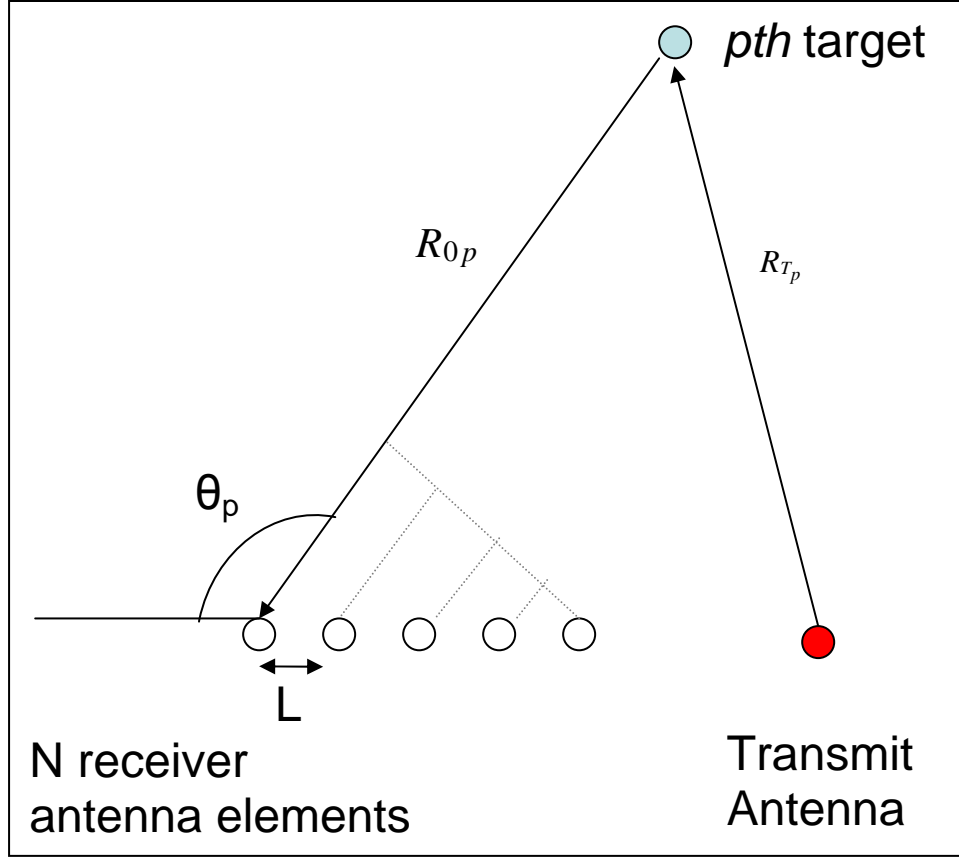


Figure 2. Two-dimensional (2-D) geometry for a 1-D linear array for a stationary target in the far-field.

For a step-frequency waveform, the returned normalized electric field from  $P$  stationary point scatter targets in the  $x$ - $y$  plane is given by

$$E(m) = \sum_{p=1}^P \sum_{n=0}^{N-1} A_p e^{-j \left[ 2\pi \left( \frac{f_0 + m\Delta f}{c} \right) (R_{T_p} + r_p(n)) \right]} \quad (1)$$

where  $E(m)$  is the normalized electric field for the  $m$ th frequency (0 to  $M-1$ ),  $p$  is the target number (1 to  $P$ ),  $n$  is the antenna element number (0 to  $N-1$ ),  $A_p$  is the amplitude associated with

the  $p$ th target,  $f_0$  is the carrier frequency, and  $\Delta f$  is the frequency step size,  $c$  is the speed of light.  $R_{Tp}$  is the range from the transmit antenna to the  $p$ th target and

$$r_p(n) = R_{0p} + nL \cos \theta_p + d_n + K \quad (2)$$

is the range from the  $p$ th target to the ADC for the  $n$ th antenna element.  $R_{0p}$  is the range from the left most receive antenna element in the array to the  $p$ th target,  $L$  is the separation between antenna elements in a linear array, and  $\theta_p$  is the angle to the  $p$ th target from the receive antenna. Finally,  $d_n$  is length of the  $n$ th delay line and  $K$  is an arbitrary constant.

From measurements of  $E(m)$ , one can estimate the angle of arrival,  $\theta_p$ , for each target. A standard approach to estimating  $\theta_p$  is to use a bank of matched filters. The matched filter output can be described as an inner product between the measured data and the selected matched filter as shown below

$$A(\theta_q) = \langle E(m), W_{\theta_q}(m) \rangle, \quad (3)$$

where  $W_{\theta_q}(m)$  is the normalized electric field for a single point target at an angle of  $\theta_q$ , range of zero and calculated using equation 1. It is desired to have the maximum response in equation 3 when the data and the matched filter are at the same angles and zero when they are at significantly different angles. The response of the match filter calculated for the  $p$ th target before the summation over frequency is given by

$$\sum_{m=0}^{M-1} E(m) W_{\theta_q}^*(m) = C \sum_{m=0}^{M-1} \left[ \left[ \sum_{n=0}^{N-1} e^{-j2\pi \left( \frac{f_0 + m\Delta f}{c} \right) (R_{Tp} + R_{0p} + nL \cos \theta_p + d_n + K)} \right] \left[ \sum_{n=0}^{N-1} e^{-j2\pi \left( \frac{f_0 + m\Delta f}{c} \right) (nL \cos \theta_q + d_n)} \right]^* \right] \quad (4)$$

where  $C$  is a constant and  $*$  is the complex conjugate. After some algebraic manipulation of equation 4, we obtain the following:

$$\begin{aligned}
\sum_{m=0}^{M-1} E(m) w_{\theta_q}^*(m) &= C \sum_{m=0}^{M-1} e^{j2\pi \left( \frac{f0 + m\Delta f}{c} \right)} (R_{\tau_p} + R_{0p}) \\
&\left( \begin{aligned}
&\sum_{n=0}^{N-1} e^{j2\pi \left( \frac{f0 + m\Delta f}{c} \right)} \left( L(\cos \theta_p - \cos \theta_q) n \right) + \\
&2 \sum_{n=0}^{N-2} e^{j2\pi \left( \frac{f0 + m\Delta f}{c} \right)} \left( L(\cos \theta_p - \cos \theta_q) n + (d_n - d_{n+1}) - L \cos \theta_p \right) + \\
&2 \sum_{n=0}^{N-3} e^{j2\pi \left( \frac{f0 + m\Delta f}{c} \right)} \left( L(\cos \theta_p - \cos \theta_q) n + (d_n - d_{n+2}) - 2L \cos \theta_p \right) + \\
&\vdots \\
&e^{j2\pi \left( \frac{f0 + m\Delta f}{c} \right)} \left( (d_0 - d_{N-1}) - (N-1)L \cos \theta_p \right)
\end{aligned} \right) \quad (5)
\end{aligned}$$

Ideally, the terms on the left-hand side of equation 5 should add to zero or near zero for  $\theta_p \neq \theta_q$ . This would result in a beam pattern with no or small sidelobes. Now, the problem is to select optimal lengths for the delay lines to minimize the sidelobes calculated from equation 5.

Obtaining this goal is a complex nonlinear problem. One approach is to use delay lines with a random statistical distribution, and then find solutions that minimize the expected value of a cost function. Using this approach, it is observed that the first term in equation 5 is independent of the delay line length, so its expected value cannot be set to zero by randomly varying the lengths of the delay line. An unbiased solution can be obtained by selecting the probability distributions of the delay lines so that the bias from the remaining terms in equation 5 cancels the first term. However, the realization of this solution is not obvious.

Another solution is to ignore the bias created by the first term and then statistically minimize the contributions from the remaining terms. A simpler criterion to optimize the length of the delay lines is to minimize the expected value of the power in the side lobes from the matched filter processing. The expected value of the contributions from all the terms, except the first, will be zero if the probability distributions of the phase differences caused by the random delays are uniformly distributed from 0 to  $2\pi$  for all combinations. However, this distribution is not realizable in hardware. If the delay lines are very long, the distributions will be approximately uniformly distributed due to the modulation of the phase by  $2\pi$ . This occurs when the length of the delay lines satisfies

$$(d_n - d_m) \Delta f / c \gg 1 \quad (6)$$

where  $n=0, \dots, N-1$  and  $m=0, \dots, N-1$  for all  $m$  and  $n$  except when  $m=n$ . This is not a requirement, but should provide a best-case scenario for an approach based on statistical optimization. This setup results in sidelobe levels (SL) proportional to

$$\begin{aligned}
SL &= \sum_{m=0}^{M-1} \sum_{n=0}^{N-1} e^{j2\pi \left( \frac{f_0 + m\Delta f}{c} \right) (L(\cos \theta_p - \cos \theta_q) n)} \\
SL &= \sum_{m=0}^{M-1} \left( \frac{1 - e^{j2\pi \left( \frac{f_0 + m\Delta f}{c} \right) L(\cos \theta_p - \cos \theta_q) N}}{1 - e^{j2\pi \left( \frac{f_0 + m\Delta f}{c} \right) L(\cos \theta_p - \cos \theta_q)}} \right) \\
SL &= C \sum_{m=0}^{M-1} \left( \frac{\sin(\pi \left( \frac{f_0 + m\Delta f}{c} \right) L(\cos \theta_p - \cos \theta_q) N)}{\sin(\pi \left( \frac{f_0 + m\Delta f}{c} \right) L(\cos \theta_p - \cos \theta_q))} \right)
\end{aligned} \tag{7}$$

and a signal strength proportional to NM. This result is complicated and is difficult to visualize. Thus, I ran simulations to gain more insight into the problem.

I used Monte Carlo simulations to investigate the impact of the line lengths on the 1-D antenna pattern using two approaches. The first approach is based on match filter processing as previously described. The second approach for estimating the angle of a target is based on minimizing the weighted squared error between a desired response and a calculated response. The weighted squared error in integral form is given by

$$\varepsilon = \int_{-\pi/2}^{\pi/2} \left| \beta_d(\theta) - s^H v(\theta) \right|^2 \Gamma(\theta) d\theta \tag{8}$$

where

$$v(\theta) = \sum_{n=0}^{N-1} e^{-jk(nL \cos \theta + d_n)}, \tag{9}$$

$$k = \frac{2\pi(f_0 + m\Delta f)}{c}, \tag{10}$$

and  $B_d(\theta)$  is the desired antenna pattern,  $\theta$  is the azimuth angle,  $s$  is a vector of beam forming coefficients,  $\Gamma(\theta)$  is the single element pattern for a radiator, and  $v(\theta)$  is a  $M \times 1$  array manifold vector that is a function of frequency step number rather than antenna element number (6). The error is minimized by breaking the integral in equation 8 into a summation over  $I$  intervals, and then approximating each interval as a single digital sample. Now, the solution to minimizing the weighted squared error is given by

$$s = \left( H^T W H \right)^{-1} H^T W, \tag{11}$$

where

$$H = \begin{bmatrix} v(\theta_1) & v(\theta_1) & \dots & v(\theta_1) \end{bmatrix}, \tag{12}$$

and  $W$  is a diagonal matrix with elements given by  $\Gamma(\theta_i)$  (7).

---

## 4. Simulation

---

I performed simulations to investigate the 1-D antenna patterns of stationary targets and the cost function of moving targets. I selected the parameters for the simulation based on the competing goals of having a low-cost system and near orthogonal antenna patterns. Simulations were performed with a carrier frequency of 10 GHz, a bandwidth of 1 GHz, 64 frequency steps, 64 antenna elements with  $\lambda/2$  antenna element spacing and Gaussian beam patterns centered at broadside with one-way 3-dB beamwidths of  $120^\circ$ , and delay lines lengths that were randomly selected with a uniform distribution between 0 and  $20\lambda$ . Figure 3 shows the antenna patterns for the first frequency at 10 GHz, the second frequency which is incremented by 15.6 MHz, and the fifth frequency, which is incremented by  $4 \times 15.6$  MHz.

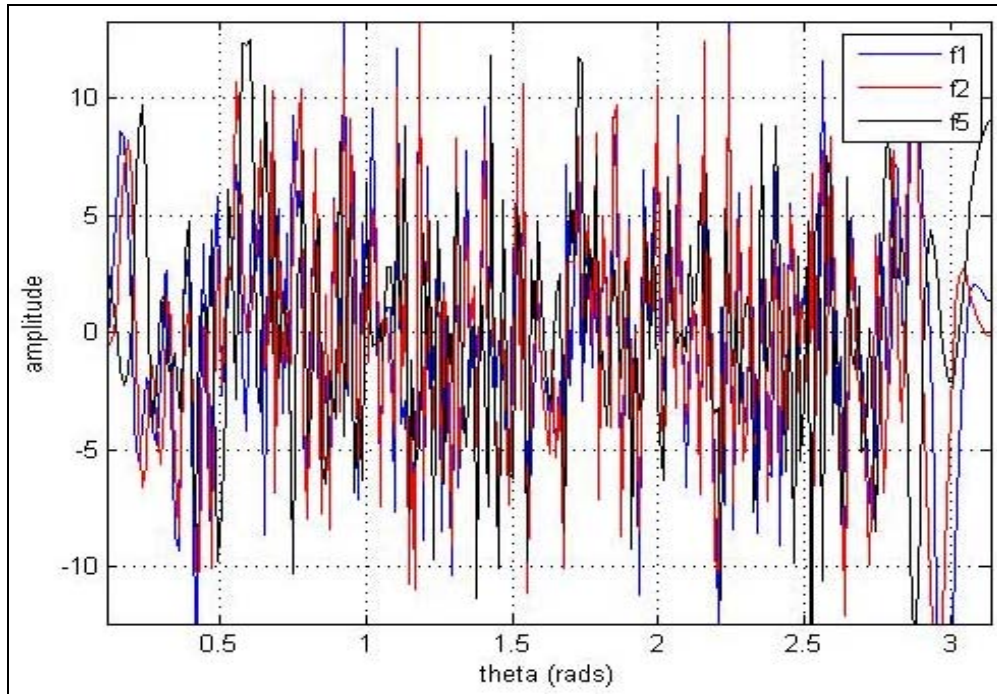


Figure 3. The 1-D receive antenna patterns for the first, second, and fifth frequency step.

The orthogonality of the antenna patterns can be analyzed by performing a single value decomposition (SVD) on the observation matrix calculated in equation 12. Figure 4 show the eigenvalues associated with the simulation parameters. The results indicate that eigenvalues are near zero around the 30<sup>th</sup> eigenvalue. Clearly, the antenna patterns are not orthogonal. The rank of the matrix can be improved by using more elements, longer delay lines, and more bandwidth, but it is never full ranked for a realizable system.

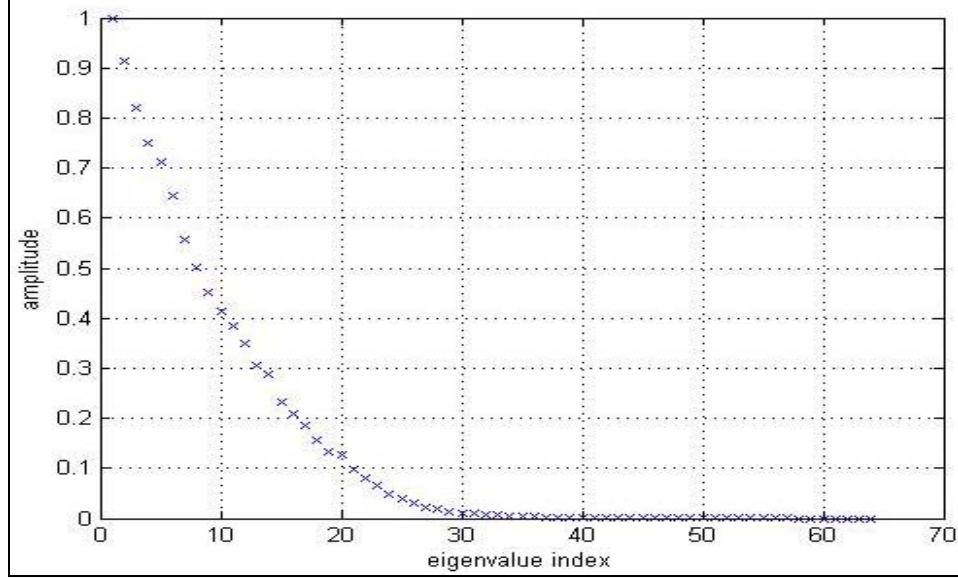


Figure 4. Eigenvalues of the observation matrix created from the different antenna patterns.

One-dimensional antenna patterns were simulated using algorithms based on matched filter processing and weighted least squares (WLSQ). The matrices required for the WLSQ fit were generated by sampling the array manifold vector in angle every  $\pi/512$  radians and the matrix inverse was computed in MATLAB using the pseudo inverse function. The results are shown in figure 5. The red curve shows the results for a WLSQ fit to the desired antenna pattern shown by the blue curve, and the black curve is generated using conventional or a matched filter approach. As expected, the sidelobes are high.

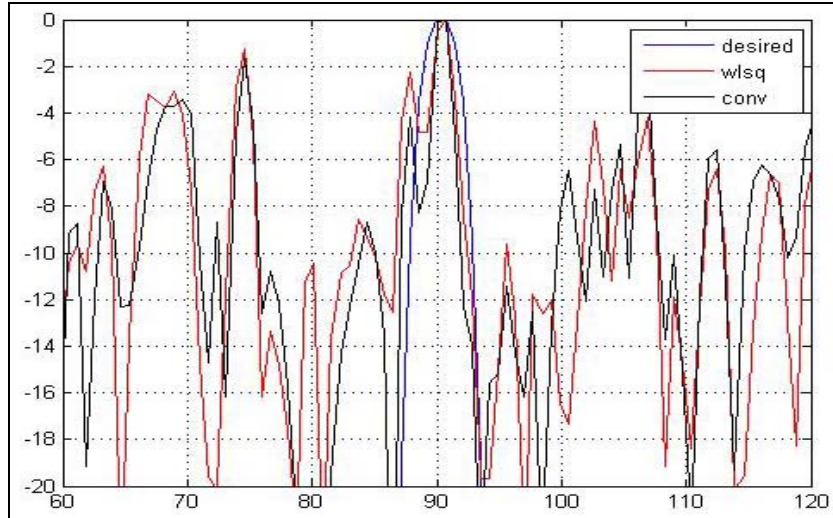


Figure 5. Simulated 1-D antenna pattern using matched filter and WLSQ approaches.

The sidelobes levels in the antenna patterns can be reduced using adaptive digital signal processing techniques that do not distort the desired signal response while minimizing the signals from another direction. Mathematically, these conditions are described using

$$w^H V(\theta_0) = 0 \quad (13)$$

$$\frac{w^H V(\theta_d)}{\|V(\theta_d)\|} = 1 \quad (14)$$

where  $\theta_d$  is the desired angle,  $\theta_0$  is the desired null angle, and  $\| \cdot \|$  is the Euclidian norm. The corresponding filter coefficients can be calculated by projecting the unconstrained solution or the matched filter solution on to the subspace constrained by equation 13 [6 – van trees]. The corresponding projection matrix is given by

$$P_{\theta_0} = V(\theta_0)[V(\theta_0)^H V(\theta_0)]^{-1} V(\theta_0)^H \quad (15)$$

and the resulting coefficients are given by

$$w_j^H = V(\theta_d)(I_M - P_{\theta_j}). \quad (16)$$

These equations will reduce the sidelobe level at a desired angle. To reduce all the significant sidelobes, the null angle can be scanned while keeping the desired angle fixed, and then finding the minimum response as shown below:

$$Y(\theta) = \min |w_j^H V(\theta)|, \quad j = 1 \dots J. \quad (17)$$

where  $w_j$  are the coefficients calculated for the  $j$ th null angle and  $v(\theta)$  is a  $M \times 1$  array manifold vector for a given angle that is a function of frequency step number (8). This procedure requires that only one signal be present. For applications where the targets are sparse and the signals can be separated in Doppler, this may be a reasonable assumption. If there is more than one target, then the additional targets need to be located, and then nulled, before the new target is detected. This process requires an additional degree of freedom for each additional target and slightly degrades the performance of the algorithm. The results from figure 5 were reprocessed using equation 17.

One-dimensional antenna patterns were simulated for signal-to-noise ratios (SNRs) of 10, 20, and 25 dB, as shown in figures 6 and 7. The SNRs were calculated for a single antenna element. The array of null angles went from  $-\pi/2$  to  $\pi/2$  in  $\pi/256$  increments, with the region at the desired angle  $\pm \pi/128$  excluded. The antenna patterns were calculated at angles going from  $-\pi/2$  to  $\pi/2$  in  $\pi/256$  increments, but were offset by  $\pi/512$ .

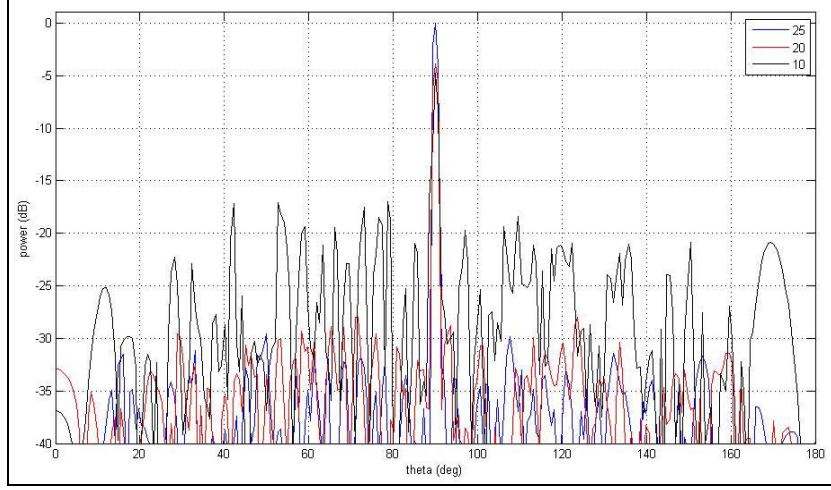


Figure 6. The 1-D antenna patterns simulated for SNRs of 10, 20, and 25 dB.

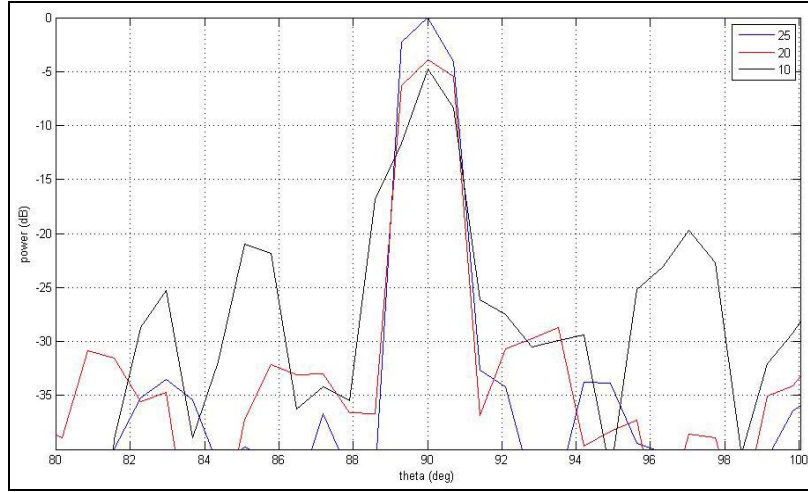


Figure 7. Zoomed in 1-D antenna patterns simulated for SNRs of 10, 20, and 25 dB.

The results indicate that the maximum peak sidelobe level is  $\sim 15$  dB below the signal of interest for an SNR of 10 dB. The performance improves with an increasing SNR. The Rayleigh criterion for angular resolution for a linear array at broadside is given by

$$\Delta\theta = \left( \frac{c}{L(f_0 + B/2)} \right) \quad (18).$$

For the parameters selected, this corresponds to an angular resolution of  $\sim 0.03$  radians or  $1.7^\circ$ . This angular resolution was almost achieved in the plots shown in figure 7.

The simulation results indicate that reasonable 1-D patterns can be generated for stationary targets. The sidelobe levels in the 1-D patterns improve as the number of elements and the fractional bandwidth is increased. The performance also improved as the number of frequencies

is increased, but levels off as it approaches the number of antenna elements. For the parameters selected, reasonable sidelobe levels required a relatively high SNR.

---

## 5. Cost Function

---

A radar system based upon this architecture needs to detect, and then estimate the location and velocity of targets in its field of view. The relationship between the parameters required for tracking and the target returns is complex and cannot be estimated using conventional radar signal processing algorithm. The estimation problem can be formulated as a nonlinear optimization problem of a cost function. The cost function can be minimized using a variety of techniques depending upon the application. Genetic algorithms, simulated annealing, or particle swarm algorithms can be used to minimize cost functions with multiple local minimums (9). These techniques can be combined with traditional approaches such as gradient descent, Newton's method, or the Nelder-Mead method once the global minimum is located (10).

One possible cost function to minimize the Euclidian or  $L_2$ -norm is

$$\min(A_p, \vec{x}_p, \vec{v}_p, \phi_p) \left\{ \left\| D(m, k) - \sum_{p=1}^P \hat{D}(m, k, A_p, \vec{x}_p, \vec{v}_p, \phi_p) \right\| \right\} \quad (19)$$

where  $A_p$  is the amplitude of the  $p$ th scattering center,  $\vec{x}_p$  is the position of the  $p$ th scattering center,  $\vec{v}_p$  is the velocity of the  $p$ th scattering center,  $\phi_p$  is the phase of the  $i$ th scattering center,  $P$  is the total number of target scattering centers,  $D(m, k)$  is the DFT of  $n$  data values measured at the  $m^{th}$  frequency step,  $k$  is the Doppler bin number, and  $\hat{D}(m, k, A_p, \vec{x}_p, \vec{v}_p, \phi_p)$  is the predicted value of  $D(m, k)$ . This is a complicated optimization problem, but for some applications, the number of targets in each Doppler bin should be zero or one, and for many applications there is only one or a few scattering centers per target. This should simplify the problem considerably.

Two-dimensional slices of the cost function described in equation 19 were generated for a target with an initial position of (5, 0) m and a velocity of (15, 15) m/s in the  $x$ - $y$  plane, with no phase offset, acceleration, or noise using the same radar parameters as previously described for the 1-D antenna simulation. Two-dimensional slices of the cost functions are plotted in figures 8 through 11 as a function of position and velocity, while the other parameters are fixed at their correct values. The plot increments are at 0.8 of the theoretical range and velocity resolution derived from the Rayleigh criterion.

The theoretical angular resolution for a stationary target given by the Rayleigh criterion is by

$$\Delta\theta = \left( \frac{c}{L \cos(\alpha) (f_0 + B/2)} \right) \quad (20)$$

where  $\alpha = \arctan(0/5) = 1$ . The figures are plotted at increments given by

$$\Delta x = 0.8 \left( \frac{c}{2B} \right) \quad (21)$$

$$\Delta y = 0.8 (r \Delta \theta) \quad (22)$$

$$\Delta V = 0.8 \left( \frac{\lambda}{4T} \right) \quad (23)$$

where  $c$  is the speed of light,  $B$  is the bandwidth of the transmitted signal,  $r$  is the range (5 m), and  $T$  is the time for each step-frequency waveform.

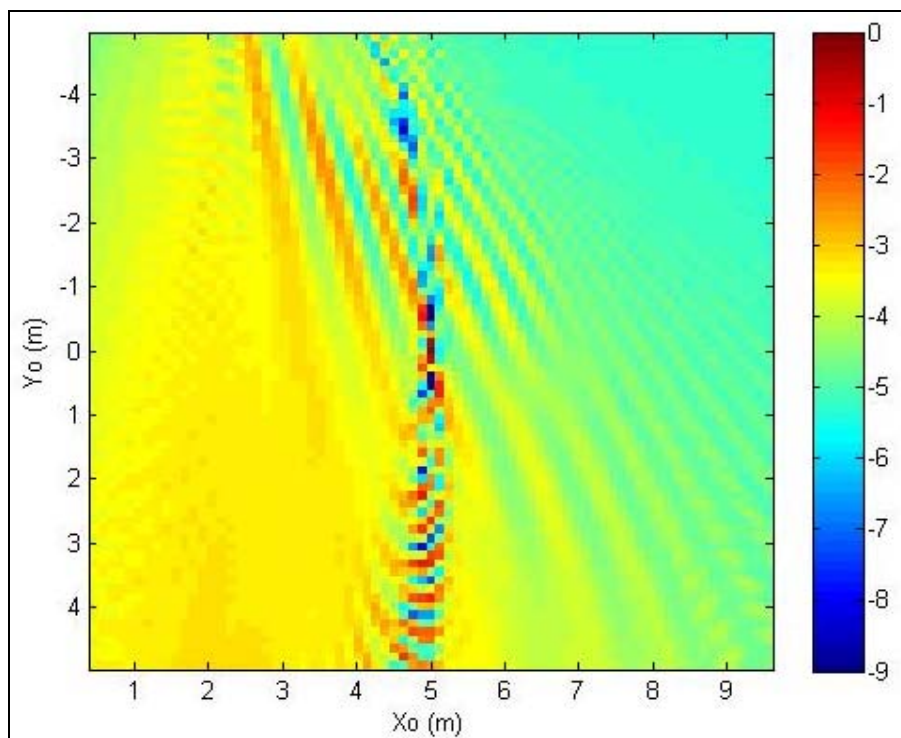


Figure 8. Cost function for a single target located at (5,0) m.

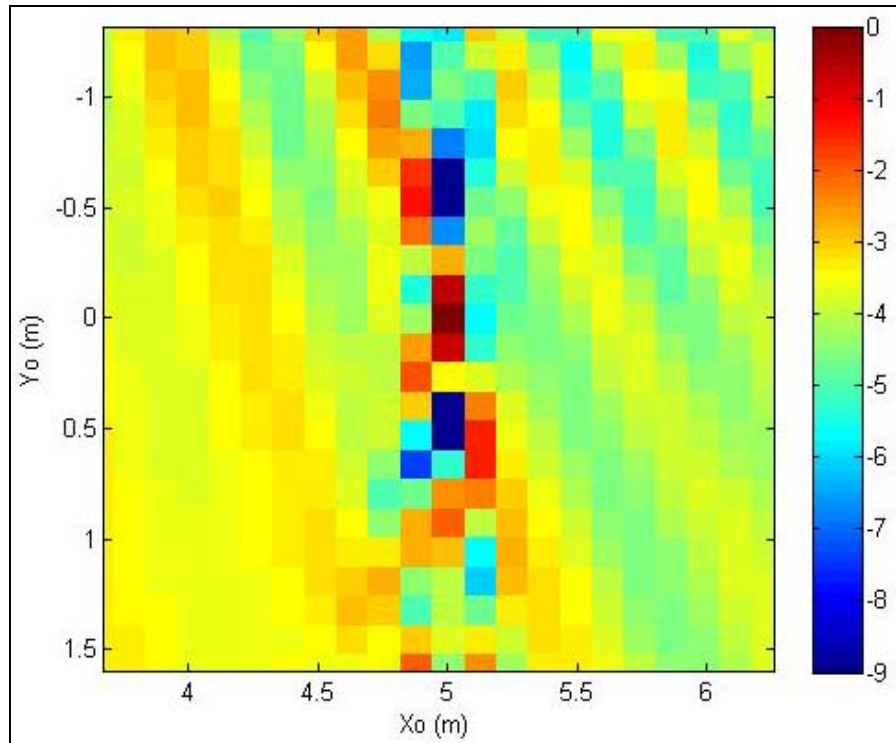


Figure 9. Cost function zoomed in for a single target located at (5,0) m.

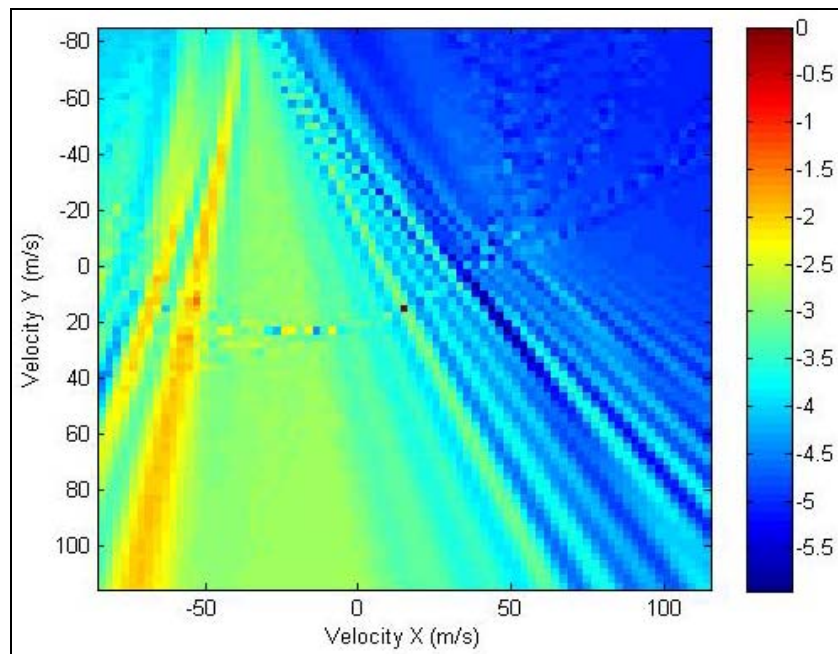


Figure 10. Cost function for a single target with a velocity vector of (15,15) m/s.

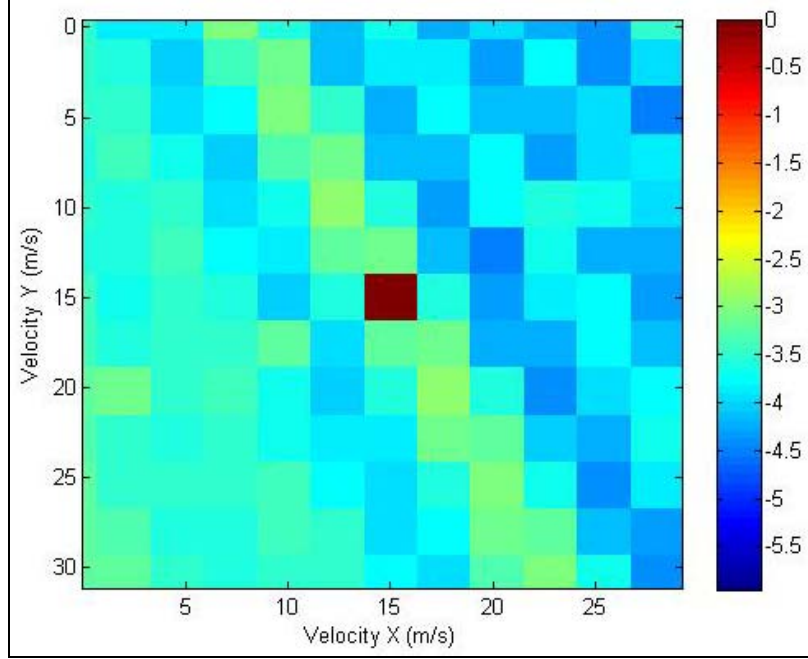


Figure 11. Cost function zoomed in for a single target with a velocity vector of (15,15) m/s.

For these simulated parameters, the target is clearly localized in velocity and downrange with resolution equal to the Rayleigh criteria, but the minimum associated with the cross-range position of the target has a relatively low separation between competing local minimums. The localization of the cross-range position will be more sensitive to noise, but the global minimum is centered around the correct value and is slightly wider than the value predicted by the Rayleigh criteria. This result is expected, since the stationary 1-D antenna patterns also had large sidelobes. The sidelobes of the cost function plots can be improved by changing the radar and waveform parameters. Increases in the percent bandwidth of the waveform, the length of the time delays, and the number of elements will reduce the sidelobes in the plots of the cost functions. Also, performance improvements can be achieved by extended this concept from a single array with one ADC to multiple subarrays with a dedicated ADC for each subarray. These results indicate that it is possible to estimate the position and velocity of a point scatter target from 2-D slices of the proposed cost function with resolution close to the Rayleigh criterion.

---

## 6. Conclusions

---

A simple radar architecture with a single input and single output was developed that supports three-dimensional (3-D) electronically scanning of moving targets with high spatial resolution. The architecture is based on a frequency scanning antenna with random length feed lines. In this study, I investigated the feasibility of the architecture to perform target localization in position and velocity by analyzing 1-D antenna patterns and a cost function based upon an  $L_2$ -norm. A

single realization of the system was selected, simulated, and analyzed. The results indicate that the concept is feasible, but requires a high SNR and complex signal processing.

For the selected parameters, the 1-D antenna patterns generated using matched filter and weighted least squares processing had high sidelobe levels. To improve the results, the sidelobes were nulled over all angles except the desired angular region. A final antenna pattern was formed by taking the minimum value of each antenna pattern at every angle. This resulted in antenna patterns with a resolution predicted by classical array theory, but it required increased signal processing and was susceptible to interference by other targets. Two-dimensional patterns can be generated using the same techniques.

Target localization will require nonlinear optimization of a cost function. Two-dimensional slices of a cost function based upon an  $L_2$  norm indicated that global minimum exists for localizing simple targets. However, the  $y$ -position estimate had a relatively small separation between other competing local minimums. The range and velocity resolution seen in the plots of the cost function were consistent with the range and velocity resolution calculated from the Rayleigh criterion.

For the system to be practical, the solution to the localization algorithm should be calculated from the radar platform. Doppler detections that exceed a given threshold could be wirelessly transmitted to a central computer for more processing. This process would reduce the cost, size, and power requirements of the radar front end. The power, size, and cost of the central computer system would be larger than traditional radar systems, but it could serve multiple roles and be located in a secure location with adequate resources.

---

## 7. References

---

1. Skolnik, M. I. *Introduction to Radar Systems*; McGraw-Hill: New York, 1981.
2. Ishimaru, A.; Tuan, H. S. Theory of Frequency Scanning Antennas. *IRE Trans. Antennas Propag.* **Mar. 1962**, *10*.
3. Bernhard, J. T.; et al. Wideband random Phased Arrays: Theory and Design. *Wideband and Multi-band Antennas and Arrays*, 2005, IEE 2005.
4. Lo, Y. T. A mathematical theory of antenna arrays with randomly spaced elements. *IEEE Trans. on Antennas and Prot.* **Mar 1964**, *12*, 257–268.
5. Shannon, C. E. A Mathematical Theory of Communication. *Bell System Technical Journal* **July, October, 1948**, *27*, 379–423, 623–656.
6. Van Trees, H. L. *Optimal Antenna Design Part IV*; Wiley Interscience: New York, 2002.
7. Kay, S. M. *Fundamentals of Statistical Signal Processing: Estimation Theory*; Prentice-Hall, 1993.
9. Avriel, Mordecai. *Nonlinear Programming: Analysis and Methods*; Dover Publishing, 2003.
10. Nelder, J. A.; Mead, R. *Computer Journal* **1965**, *7*, 308–313.

---

## List of Symbols, Abbreviations, and Acronyms

---

1-D	one-dimensional
2-D	two-dimensional
3-D	three-dimensional
ADC	analog-to-digital converter
BPF	band-pass filter
CW	continuous wave
DFT	discrete Fourier transform
ESA	electronically scanning antenna
MTI	moving target indicator
SL	sidelobe level
SNR	signal-to-noise ratios
SVD	single value decomposition
WSLQ	weighted least squares

NO. OF COPIES	ORGANIZATION	NO. OF COPIES	ORGANIZATION
1 ELEC	ADMNSTR DEFNS TECHL INFO CTR ATTN DTIC OCP 8725 JOHN J KINGMAN RD STE 0944 FT BELVOIR VA 22060-6218	5	US ARMY RSRCH LAB ATTN IMNE ALC HRR MAIL & RECORDS MGMT ATTN RDRL CIM L TECHL LIB ATTN RDRL CIM P TECHL PUB ATTN RDRL SER M G GOLDMAN ATTN RDRL SES P M SCANLON ADELPHI MD 20783-1198
1 CD	OFC OF THE SECY OF DEFNS ATTN ODDRE (R&AT) THE PENTAGON WASHINGTON DC 20301-3080	TOTAL: 13 (1 ELEC, 1 CD, 11 HCS)	
1	US ARMY RSRCH DEV AND ENGRG CMND ARMAMENT RSRCH DEV & ENGRG CTR ARMAMENT ENGRG & TECHNLOGY CTR ATTN AMSRD AAR AEF T J MATTS BLDG 305 ABERDEEN PROVING GROUND MD 21005-5001		
1	PM TIMS, PROFILER (MMS-P) AN/TMQ-52 ATTN B GRIFFIES BUILDING 563 FT MONMOUTH NJ 07703		
1	US ARMY INFO SYS ENGRG CMND ATTN AMSEL IE TD A RIVERA FT HUACHUCA AZ 85613-5300		
1	COMMANDER US ARMY RDECOM ATTN AMSRD AMR W C MCCORKLE 5400 FOWLER RD REDSTONE ARSENAL AL 35898-5000		
1	US GOVERNMENT PRINT OFF DEPOSITORY RECEIVING SECTION ATTN MAIL STOP IDAD J TATE 732 NORTH CAPITOL ST NW WASHINGTON DC 20402		
1	US ARMY RSRCH LAB ATTN RDRL CIM G T LANDFRIED BLDG 4600 ABERDEEN PROVING GROUND MD 21005-5066		